Analytica Chimica Acta 1057 (2019) 88–97

Contents lists available at ScienceDirect

Analytica Chimica Acta

journal homepage: www.elsevier.com/locate/aca

Q-graphene-scaffolded covalent organic frameworks as fluorescent probes and sorbents for the fluorimetry and removal of copper ions

Yuanyuan Cai, Yao Jiang, Luping Feng, Yue Hua, Huan Liu, Chuan Fan, Mengyuan Yin, Shuai Li, Xiaoxia Lv, Hua Wang*

Institute of Medicine and Materials Applied Technologies, College of Chemistry and Chemical Engineering, Qufu Normal University, Qufu City, Shandong Province, 273165, PR China

HIGHLIGHTS

- Metal-free COFs were polymerized onto the scaffolds of hollow Q-Graphene (QG).
- QG-scaffolded COFs could present enhanced fluorescence, high aqueous stability, and photostability.
- The fluorescence of QG-scaffolded COFs could be quenched by Cu^{2+} ions towards the ultrasensitive copper analysis.
- The QG-scaffolded COF could serve as powerful sorbents for the removal of Cu^{2+} ions in wastewater with high efficiency.

GRAPHICAL ABSTRACT

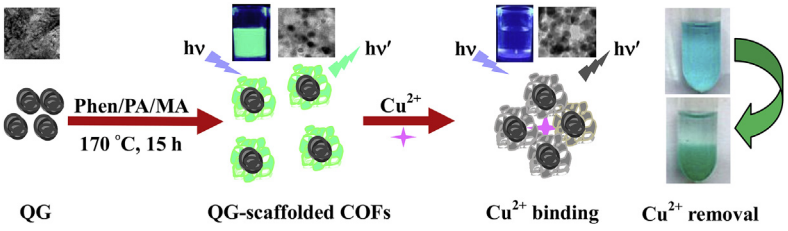

ARTICLE INFO

Article history:
Received 6 November 2018
Received in revised form
18 December 2018
Accepted 27 December 2018
Available online 9 January 2019

Keywords:
Q-graphene scaffold
Covalent organic frameworks
Fluorescent analysis
Removal sorbents
Copper ions

ABSTRACT

Metal-free fluorescent covalent organic frameworks (COFs) were synthesized initially with Q-Graphene (QG) scaffolds by the one-step covalent reactions of melamine-aldehyde and phenol-aldehyde polycondensations using paraformaldehyde. It was discovered that onion-like hollow QG, which consists of multi-layer graphene and different carbon allotropes having a high proportion of folded edges and surface defects, could endow the scaffolded COFs with enhanced green fluorescence and environmental stability. Unexpectedly, they could exhibit the powerful absorption for Cu^{2+} ions resulting in the specific quenching of fluorescence. A fluorimetric strategy with QG-scaffolded COFs was thereby developed to probe Cu^{2+} ions separately in blood and wastewater with the linear concentration ranges of 0.0010 −10.0 μM (limit of detection of 0.50 nM) and 0.0032−32.0 μM (limit of detection of 2.4 nM), respectively, promising the potential applications for the field-applicable monitoring of Cu^{2+} ions in the clinical and environmental analysis fields. In addition, the prepared COFs sorbents were employed to absorb Cu^{2+} ions in wastewater showing high removal efficiency. More importantly, such an one-pot fabrication route with hollow QG scaffolds may be tailorable extensively for the preparation of a variety of metal-free multifunctional COFs with enhanced fluorescence, water solubility, environmental stability, and metal removal capability.

1. Introduction

It is well established that copper (Cu) as a trace element plays a

* Corresponding author.
E-mail address: huawang@qfnu.edu.cn (H. Wang).
URL: http://wang.qfnu.edu.cn

https://doi.org/10.1016/j.aca.2018.12.054
0003-2670/

vital role in a variety of important physiological activities in human body such as metabolism, growth, and immune system development [1]. Clinical studies have shown that Cu^{2+} ions deficiency can cause some serious diseases; however, too high concentrations of this heavy metal in body fluids like blood can also have some harmful effects. Additionally, the long-term exposure to high-level Cu^{2+} ions in environmental water like wastewater can bring about cellular toxicity [2] and organ damage [3], although Cu^{2+} ions possess some important functions in nature such as the promotion for the growth of plants [4]. Therefore, it is of practical interest to valuate Cu levels in human fluids like blood and environmental wastewater including the removal of Cu^{2+} ions.

Up to date, many classic instrumental analysis methods have been developed to probe Cu^{2+} ions, most known as the atomic absorption spectrometry [5], inductively coupled plasma mass spectrometry [6], X-ray spectroscopy [7], and fluorimetric analysis methods [8,9]. Among these techniques, the fluorescence (FL) analysis method has preferentially applied for detecting the biomarkers including some heavy metal cations like Cu^{2+} ions [10]. Since the fluorimetric analysis performances are well recognized to depend on the optical properties of fluorescent probes like quantum yield and aqueous stability, various modern fluorescent materials have prepared for the fluorimetric applications, typically including quantum dots [11] and organic dyes [12]. Yet, they may encounter with some challenges such as low fluorescent intensity, heavy metal toxicity, and environmental instability. Therefore, developing some new fluorescent probes with high luminescence, low toxicity, good stability, and especially high analyte-absorption capacity is of great importance for the large-scale fluorimetric applications.

Recent years have witnessed the rapid development of covalent organic frameworks (COFs) materials with the diverse applications for metal-free catalysis, adsorption, separation, sensors and biotechnology [13]. The versatile materials are commonly synthesized by joining the organic building units together through the strong covalent bonds, with the porous skeletons and periodic structures [14]. In contrast to the common crystalline solid materials, COFs materials are composed of only light elements showing some outstanding advantages such as low toxicity, large surface area, high stability, tunable pore structure, tailorable functionalities (i.e., FL), and especially analyte adsorption capacity [15,16]. Moreover, many efforts have recently been devoted to the applications of graphene or graphene oxides for energy storage, electrochemical sensors, and fluorescent probes [17–24]. For example, Lin's group employed graphene for the sensitive electroanalysis of glucose [18]. Wu et al. has proposed a graphene oxide-based FL analysis method to probe Pb^{2+} ions [23]. In particular, there has recently emerged another hot graphene material of Q-graphene (QG), known as carbon quantum dot or nano-onion, which is a kind of hollow nanomaterial consisting of multi-layer graphene and different types of carbon allotropes with a high proportion of folded edges and surface defects to promise the sensing applications [25,26]. For example, Banks and colleagues employed QG for the design of electrochemical sensor with promoted electron transferring.

In the present work, metal-free fluorescent QG-scaffolded COFs were synthesized for the first time by the one-step covalent reactions of melamine (MA)-aldehyde and phenol (Phen)-aldehyde poly-condensation using paraformaldehyde (PA). Herein, MA as a nitrogen-rich molecule can be readily coupled with PA by the amine-aldehyde reaction to produce the metal-free polymers serving as strong sorbent for some heavy metal ions especially Cu^{2+} ions [27]. Meantime, Phen, which is well known as a raw chemical material widely applied for preparing functional resins, fungicides [28], and drugs [29], can be bound with PA by the Phen-aldehyde poly-condensation to yield the Phen-PA resin with luminescence [30]. The two kinds of covalent reactions were thereby combined to work with hollow QG to prepare the metal-free QG-scaffolded COFs. To our surprise, the resulting COFs nanocomposites could display enhanced green FL and environmental stability, in comparison with the ones without QG scaffolds. Moreover, they could exhibit the powerful Cu^{2+} absorption capacity together with the specific FL quenching. A fluorimetric analysis method was thus developed for probing Cu^{2+} ions separately in blood and wastewater, in addition to the efficient removal of Cu^{2+} ions in wastewater. Systematic studies were conducted on the sensing and removal performances of the developed QG-scaffolded COFs for Cu^{2+} ions by using transmissions electron microscopy (TEM), FL spectrophotometer, UV–vis spectrophotometer, and FL microscopy. To the best of our knowledge, this is the first report on the QG scaffolds-based synthesis of metal-free multifunctional metal-free COFs by the one-step covalent reactions of amine-aldehyde and phenol-aldehyde poly-condensations to serve as the robust sensing probes and strong sorbents for the fluorimetry and removal of Cu^{2+} ions.

2. Experimental section

2.1. Reagents

Melamine (MA), paraformaldehyde (PA), phenol (Phen), cysteine (Cys), Glycine (Gly) and human serum albumin (HSA) were purchased from Sigma Aldrich (Beijing, China). Q-graphene (QG) materials were purchased from Graphene Supermarket (Calverton, United States). Blood samples were kindly provided by the local hospital. Anhydrous $CuSO_4$ and other inorganic salts were purchased from Beijing Chemical Reagent Co., Ltd (Beijing, China). All of the chemicals are of analytical grade. Glass containers were cleaned separately by aqua regia and ultrapure water before usage. Deionized water (>18 Mohm-cm) was supplied from an Ultra-pure water system (Pall, USA).

2.2. Apparatus

The fluorescence (FL) measurements were conducted using FL spectrophotometer (Horiba, FluoroMax-4, Japan) operated at an excitation wavelength at 420 nm, with both excitation and emission slit widths of 5.0 nm. UV-3600 spectrophotometer (Shimadzu, Japan) was used to measure the UV–vis spectra of the different functional materials including those with Cu^{2+} ions. Transmission electron microscopy (TEM, JEM-2100PLUS, Japan) imaging operated at 100 kv was employed to characterize the morphological structures of QG-scaffolded COFs before and after adding Cu^{2+} ions, including the analysis of energy-dispersive X-ray spectroscopy (EDX). Besides, the photographs of corresponding reaction products were obtained under UV light at exciting wavelength of 365 nm.

2.3. Synthesis of QG-scaffolded COFs

QG powders were first dispersed into alcohol and further screened by centrifuging, then dried in air. After that, an aliquot of QG (4.0 mg) was dispersed ultrasonically in 10 mL water for 20 min. Furthermore, an aliquot of MA (40.0 mg) was introduced into 30 mL water to be heated under the magnetic stirring. After the completion of the dissolution of MA (40.0 mg), Phen (14.1 mg) and PA (40.0 mg) were added in turn into the above solution, followed by the continuous heating for 10 min. Subsequently, an aliquot of above QG materials (0.40 mg mL^{-1}, 4.0 mL) was introduced into the mixture, and then transferred into the 50-mL Teflon-lined autoclave to be heated for 15 h at 170 °C. After the mixture was cooled down to room temperature, the products were centrifuged and

washed with water for three times, and finally stored in refrigerator. In addition, the synthesis of COFs without QG was conducted according to the procedure above, except for no addition of QG.

2.4. Fluorimetric analysis and removal tests for Cu^{2+} ions using QG-scaffolded COFs

The detection conditions of the fluorimetric assays for Cu^{2+} ions were optimized, including the QG-scaffolded COFs dosages (1.0, 2.0, 3.0, 4.0, 5.0, and 6.0 mg mL^{-1}), pH values (1.0, 3.0 5.0, 7.0, 9.0, 11.0, and 13.0), ionic strengths (0.0, 50, 100, 200, 300, and 400 mM NaCl), and response time (1.0, 2.0, 3.0, 4.0, 5.0, and 6.0 min). Moreover, the control tests for different metal cations of 1.0 μM (Cu^{2+}, Pb^{2+}, Mg^{2+}, Hg^{2+}, Zn^{2+}, Fe^{2+}, Fe^{3+}, Co^{2+}, Cd^{2+}, Cr^{3+}, Ni^{2+}, K^{+}, Ca^{2+}, and Na^{+} ions), and amino acids (Gly and Cys) (10.0 μM) and HSA (50.0 mg mL^{-1}) were separately conducted. Herein, the quenching efficiencies were calculated according to the following equation: quenching efficiencies (percentages) = $(F_0 - F)/F_0$ x 100%, where F_0 and F refer to the FL intensities of the QG-scaffolded COFs in the absence and presence of Cu^{2+} ions, respectively.

Under the optimized conditions, the fluorimetric assays with QG-scaffolded COFs were applied for probing Cu^{2+} ions spiked separately in blood or wastewater samples. An aliquot of QG-scaffolded COFs (4.0 mg mL^{-1}) was separately mixed with a certain amount of Cu^{2+} ions of different concentrations spiked in blood (0.0010, 0.0050, 0.010, 0.050, 0.10, 0.50, 1.0, 5.0, and 10.0 μM). The fluorimetric measurements were then performed by recording the changes of FL intensities. In addition, the Cu^{2+}-removal experiments were performed using QG-scaffolded COFs of various amounts for the adsorption of Cu^{2+} ions with different levels in wastewater samples, of which the changes of absorbance values of Cu^{2+} solutions were recorded to calculate the removal efficiencies (percentages).

3. Results and discussion

3.1. Main synthesis procedure and Cu^{2+}-sensing mechanism of QG-scaffolded COFs

Scheme 1 schematically illustrates the main synthesis procedure and sensing mechanism of metal-free fluorescent QG-scaffolded COFs for the fluorimetric analysis and absorption of Cu^{2+} ions. Herein, MA with three amino groups can be coupled with PA to yield the metal-free MA-PA composites through the amine-aldehyde reactions [27,31]. Meanwhile, Phen can be bound with PA to produce Phen-PA resin through the Phen-aldehyde polycondensation [32]. As manifested in Scheme 1A, the two kinds of covalent reactions were initially combined to prepare COFs, but showing a weak fluorescence (FL) and poor environmental stability. Alternatively, hollow QG was introduced to act as the scaffolds for COFs in the one-pot reactions (Scheme 1B). To our surprise, the resulting metal-free COFs could display enhanced green FL, aqueous solubility, and environmental stability, in contrast to the ones without QG scaffolds above. What is more, they could exhibit the powerful Cu^{2+} absorption capacity, together with the specific Cu^{2+}-quenching FL. Herein, on the one hand, the Phen-PA resin of QG-scaffolded COFs can enjoy an internal network of three-dimensional crosslinks as described in Scheme 1A, which may conduct the fast absorption kinetics for Cu^{2+} ions. Meantime, the metal-free MA-PA composites composed in the QG-scaffolded COFs might possess the large surface area and especially rich inherent aminals (−NH−CH_2−NH−) to perform the specific binding and powerful absorption capacity for Cu^{2+} ions [33]. On the other hand, hollow QG scaffolds consisting of numerous six-membered rings can conduct the strong π-π stacking interactions with the benzene rings of MA-PA composites and Phen-PA resin, thus endowing the resulting QG-scaffolded COFs sorbents with greatly improved environmental stability against any self quenching and light bleaching. Remarkably, QG as onion-like hollow carbon nanospheres with multilayer graphene can possess a high ratio of folded edges and surface defects so as to improve the luminescence of the COFs (the detailed mechanism would be explored in future), which can be quenched by Cu^{2+} ions as schematically revealed in Scheme 1B. A highly selective and sensitive fluorometric analysis method was thereby expected for probing Cu^{2+} ions in blood or wastewater samples, in addition to the efficient removal of Cu^{2+} ions in wastewater afterwards.

3.2. Main reaction conditions for the synthesis of QG-scaffolded COFs

The main reaction conditions were optimized for preparing the QG-scaffolded COFs to serve as the fluorescent probes and removal sorbents for Cu^{2+} ions. As shown in Fig. 1A, the most suitable MA-to-Phen ratio was found to be 15/1, at which the QG-scaffolded COFs could be fabricated with the strongest FL. Fig. 1B describes the effects of the QG amounts on the FL intensities of the resulting COFs probes. Obviously, the brightest FL probes were achieved at QG dosage of 0.40 mg mL^{-1}. Moreover, the reaction time for the synthesis of QG-scaffolded COFs was explored, indicating the maximum FL at the reaction time of 15 h (Fig. 1C). Additionally, the reaction temperature was optimized, showing the ideal one at 170 °C (Fig. 1D).

3.3. Environmental stability of fluorescent QG-scaffolded COFs probes

The environmental stability of QG-scaffolded COFs probes was investigated under the harsh testing conditions in comparison with pure COFs without QG. Fig. 2A exhibits the comparable results of optical stability for QG-scaffolded COFs by exposure to the xenon lamp over different time intervals. One can note that QG-scaffolded COFs could display no significant change of FL intensities even over different time intervals. Furthermore, QG-scaffolded COFs could interestingly display no significant change of FL intensities even exposed to the strong light up to 60 min (curve a), in contrast to pure COFs showing an apparent decrease (curve b). The storage stability of QG-scaffolded COFs in water was also studied comparably (Fig. 2B). The data indicate that QG-scaffolded COFs could basically maintain their FL intensities even stored for six months (curve a). However, there is a great decay in the FL intensities for pure COFs (curve b). Therefore, the developed QG-scaffolded COFs probes can possess much improved environmental stability against possible light bleaching and self-quenching in aqueous storage, due to that hollow QG scaffolds should perform the strong π-π stacking interactions with the benzene rings of MA-PA composites and Phen-PA resin of the conjugated COFs probes showing the greatly enhanced environmental stability.

3.4. The sensing performances of QG-scaffolded COFs for Cu^{2+} ions

It is well recognized that QG nanomaterials are hollow carbon nanospheres composing of multiple layers of graphene and high folding edges and surface defects, which has been demonstrated to ensure the rapid electron transfer kinetics [27]. Herein, QG was employed alternatively as the scaffolds for the fluorescent COFs that would be polymerized in the one-pot hydrothermal reactions to yield the fluorescent QG-scaffolded COFs. Fig. 3A shows the comparison of FL intensities between QG-scaffolded COFs and pure COFs the absence and presence of Cu^{2+} ions. As can be seen from

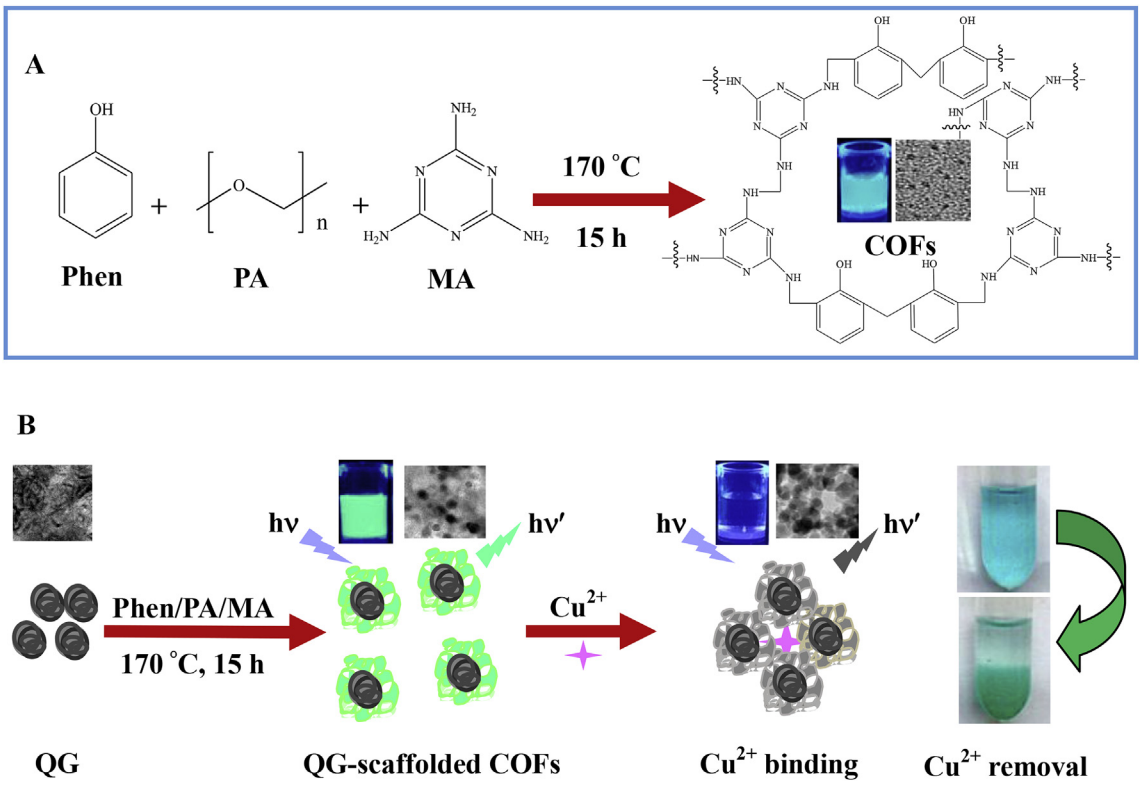

Scheme 1. Schematic illustration of (A) the covalent polymerization reaction among Phen, PA, and MA to yield COFs. (B) The fabrication and procedure of metal-free QG-scaffolded COFs by the COFs covalent reaction system with QG scaffolds, yielding the products with bright green fluorescence that could be quenched by Cu^{2+} ions and for the Cu^{2+} removal.

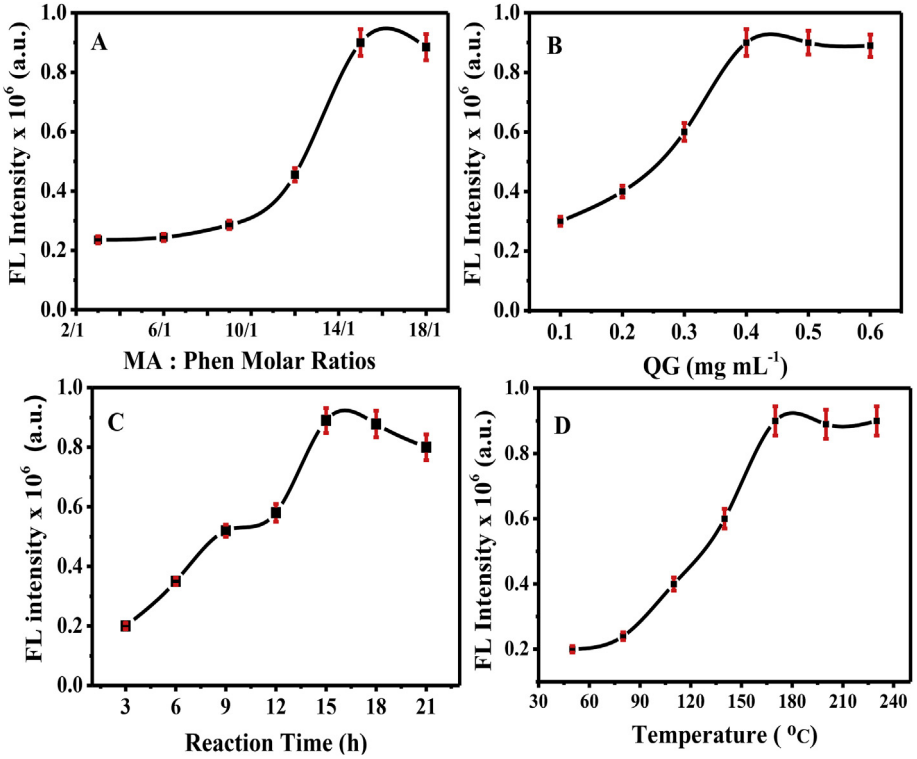

Fig. 1. Optimization of the preparation conditions for QG-scaffolded COFs including (A) the MA-Phen molar ratios, (B) QG dosages, (C) polymerization reaction time, and (D) covalent polymerization reaction temperature.

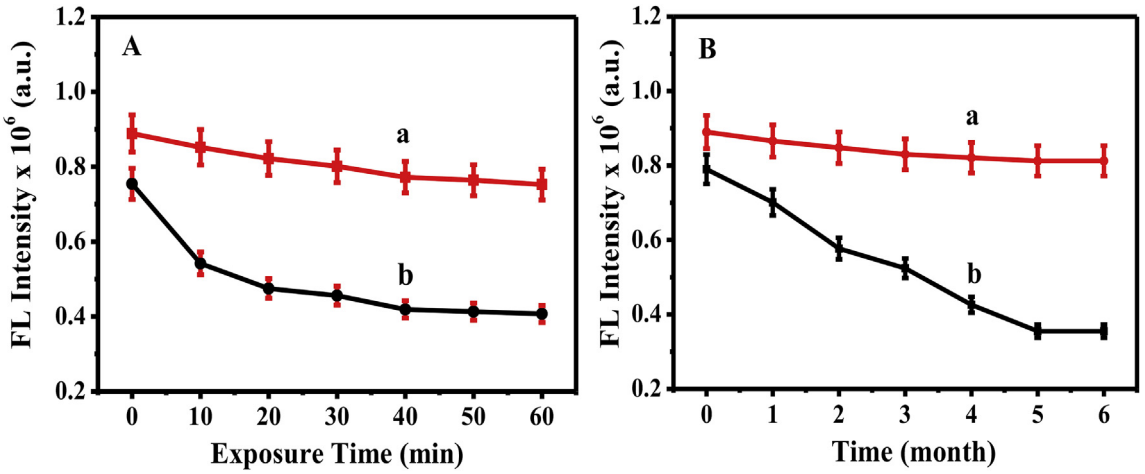

Fig. 2. Comparison of FL intensities of (a) QG-scaffolded COFs and (b) COFs depending on the (A) exposure time under xenon lamp and (B) storage time in dark at 4 °C.

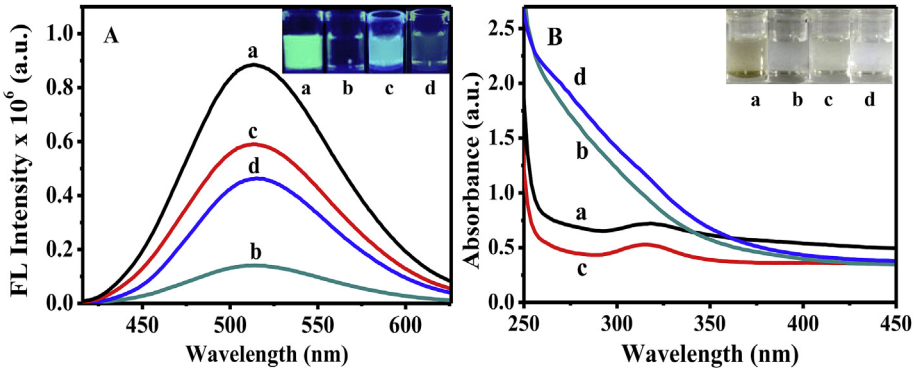

Fig. 3. (A) Fluorescence spectra and (B) UV–vis spectra of QG-scaffolded COFs in the (a) absence and (b) presence of Cu^{2+} ions, in comparison with COFs(c) without and (d) with Cu^{2+} ions (insert: the photographs of corresponding product solutions under UV or white light).

Fig. 3A, both of QG-scaffolded COFs and pure COFs could have the emission spectra peaking at 512 nm. However, the FL intensity of QG-scaffolded COFs (curve a) is about 1.5-time higher than that of pure COFs (curve c), as visually observed from their photographs (Fig. 3A, insert). Accordingly, the introduction of QG scaffolds could dramatically enhance the FL of COFs by forming QG-scaffolded COFs, in contrast to the common graphene materials that generally act as the FL quenchers [22,23]. More importantly, QG-scaffolded COFs (curve b) could obtain much greater Cu^{2+}-induced FL quenching than pure COFs (curve d). Herein, it is interesting to speculate that the FL enhancement of COFs coatings might be attributed to the high ratios of folded edges and surface defects of QG scaffolds, although the detailed reasons have not yet been clear. Furthermore, a comparison of UV–vis spectra was performed between QG-scaffolded COFs and pure COFs in the presence and absence of Cu^{2+} ions (Fig. 3B). It was found that QG-scaffolded COFs (curve a) and pure COFs (curve c) might have the same UV absorption peak at 325 nm. Interestingly, they could display no obvious peaks of UV–vis absorption in presence of Cu^{2+} ions (curve b and d). Also, there is no apparent colour change in all of the testing solutions under the visible light, as directly revealed by their photographs (Fig. 3B, insert). Yet, both QG-scaffolded COFs and pure COFs might be structurally changed after the Cu^{2+} chelation resulting in the agglomerations as evidenced in the TEM images below.

The changing morphological structures of QG-scaffolded COFs before and after adding Cu^{2+} ions were characterized by TEM imaging, taking pure COFs for the comparison (Fig. 4). One could see from Fig. 4A that QG could display the onion-like hollow profiles with varying sizes of about 20–30 nm in diameter. Moreover, pure COFs were formed as small nanoparticles with the average size of about 2.0 nm in diameter (Fig. 4B). When COFs were coated onto QG scaffolds, the resulting QG-scaffolded COFs could have the well-defined spheric nanostructures with the average size of about 30.0 nm in diameter (Fig. 4C). As expected, the QG-scaffolded COFs could desirably display the spheric nanostructures. However, after the addition of Cu^{2+} ions, QG-scaffolded COFs would be largely agglomerated (Fig. 4D). The change of their topological structures could be clearly witnessed in the corresponding high-resolution images of amplified particles (Fig. 4E and F). Also, EDX analysis was performed for the COFs with and without Cu^{2+} ions, confirming the changing chemical compositions so expected (Fig. 4G and H). Herein, Cu^{2+} ions might specifically chelate with the inherent aminals (–NH–CH_2–NH–) of MA-PA composites in QG-scaffolded COFs [33], as schematically described in Scheme 1B, thus leading to the agglomeration of the COFs. Additionally, the Phen-PA resin of QG-scaffolded COFs with three-dimensional crosslinking networks might also help to absorb Cu^{2+} ions to trigger the fast agglomeration of the COFs probes towards the FL quenching as aforementioned.

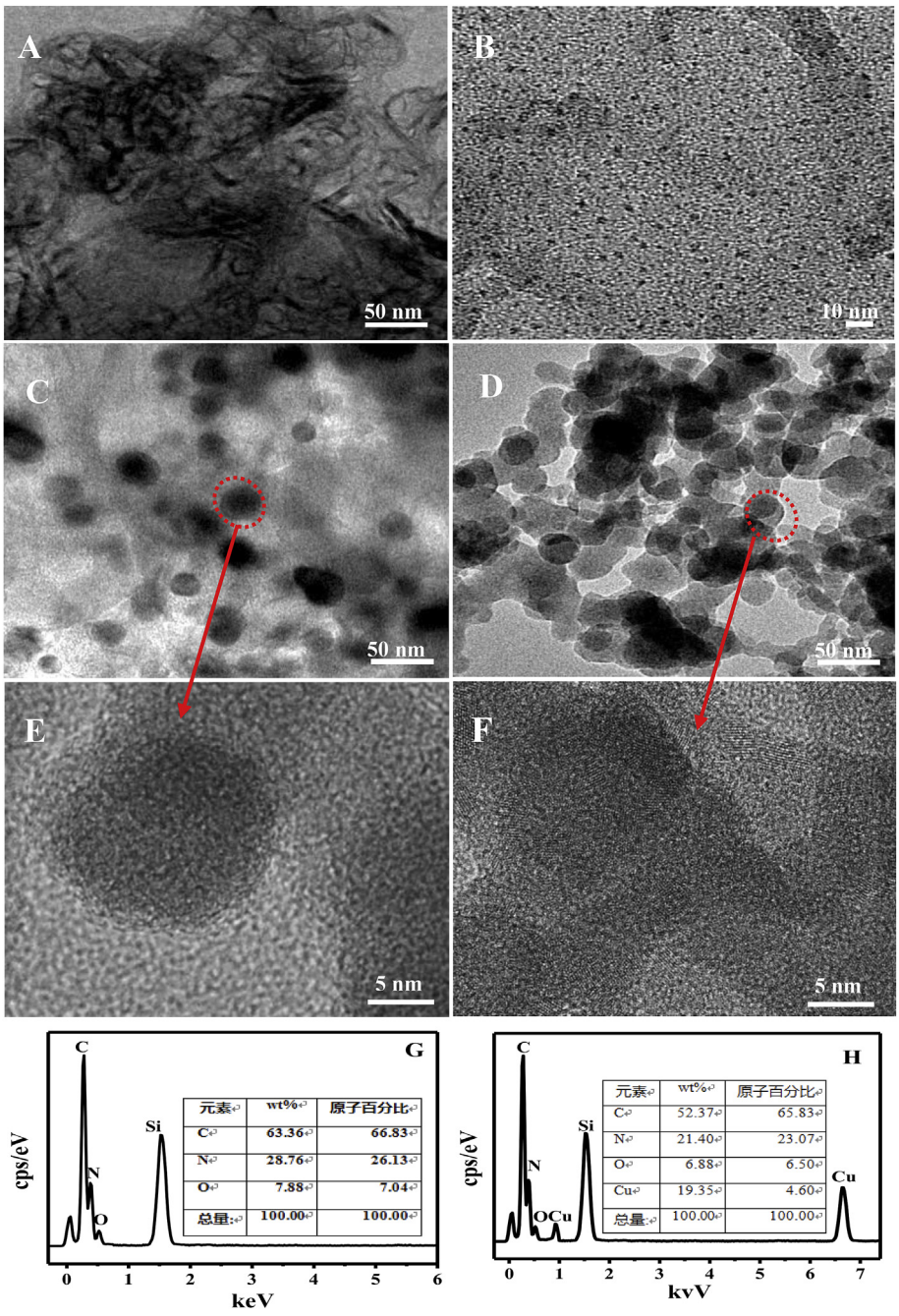

Fig. 4. TEM images of (A) QG, (B) COFs, QG-scaffolded COFs in the (C) absence and (D) presence of Cu^{2+} ions, with (E, F) the corresponding high-resolution TEM images of amplified particles, respectively; EDX analysis results of QG-scaffolded COFs in the (G) absence and (H) presence of Cu^{2+} ions.

3.5. Selective sensing and absorption tests of QG-scaffolded COFs for Cu^{2+} ions

The sensing selectivity of fluorometric responses of QG-scaffolded COFs to Cu^{2+} ions was systematically explored by comparing to some other metal cations and amino acids (i.e., Cys and Gly) and HSA (Fig. 5A). It was found that only Cu^{2+} ions could trigger the large FL quenching of QG-scaffolded COFs, as apparently witnessed in the corresponding photographs (Fig. 5A, insert). Accordingly, QG-scaffolded COFs could serve as the robust fluorescent probes for the selective Cu^{2+} detections. As aforementioned, herein, the Cu^{2+}-caused FL quenching of QG-scaffolded COFs is ascribed to the inherent aminals (−NH−CH_2−NH−) of MA-PA composites in QG-scaffolded COFs that could specifically chelate with Cu^{2+} ions [33], thus resulting in the agglomeration toward the FL quenching of the COFs probes.

The absorption capacity of QG-scaffolded COFs for Cu^{2+} ions was investigated with the results shown in Fig. 5B. One can note that QG-scaffolded COFs could conduct the rapid absorption of Cu^{2+} ions, which could be completed within about 40 s, as comparably visualized in the photographs of the testing solutions (Fig. 5B, insert). Moreover, the other conditions for Cu^{2+} adsorption were optimized (Fig. 6). As shown in Fig. 6A, the amounts of QG-scaffolded COFs could exert the apparent effects on the efficiencies of Cu^{2+} removals, showing the maximum one obtained at 9.0 mg mL^{-1} COFs (Fig. 6A). In addition, the biggest Cu^{2+}-removal

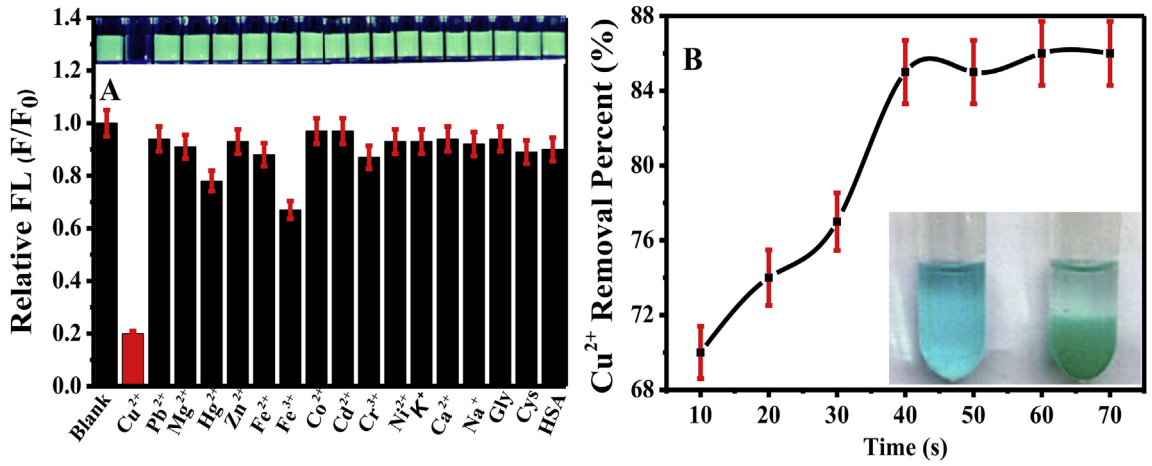

Fig. 5. (A) Relative FL responses of QG-scaffolded COFs (4.0 mg mL^{-1}) to different metal ions (1.0 μM) including Cu^{2+}, Pb^{2+}, Mg^{2+}, Hg^{2+}, Zn^{2+}, Fe^{2+}, Fe^{3+}, Co^{2+}, Cd^{2+}, Cr^{3+}, Ni^{2+}, K^{+}, Ca^{2+}, Na^{+}, and Gly(10 μM), Cys(10 μM), HSA (50 mg mL^{-1}), with the corresponding photographs of testing solutions under UV light (top). (B) The removal percentages of QG-scaffolded COFs for Cu^{2+} ions in a wastewater containing 100 mM Cu^{2+} ions, with the photographs of the Cu^{2+} solutions ions before (left) and after (right) adding QG-scaffolded COFs (4.0 mg mL^{-1}).

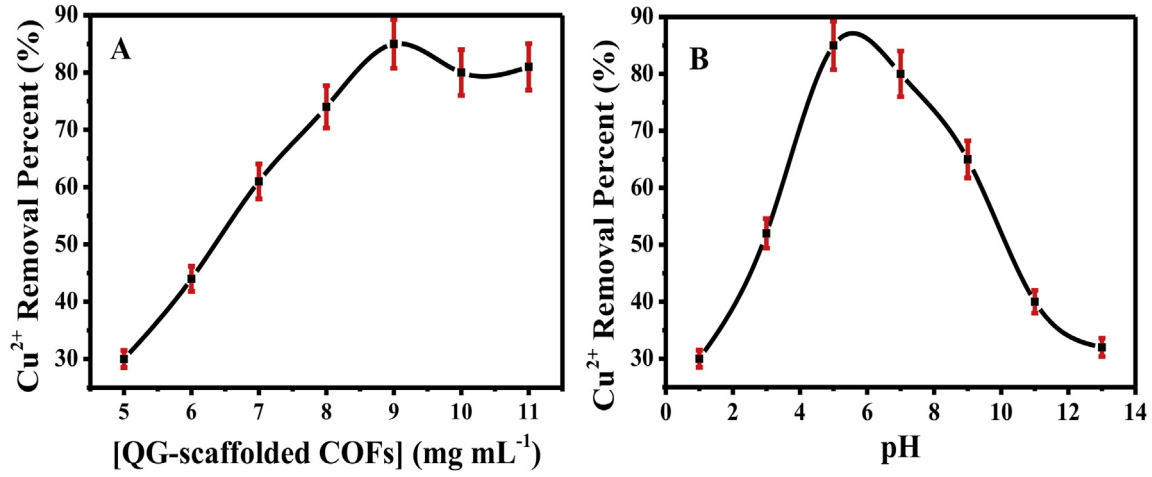

Fig. 6. The main adsorption conditions for Cu^{2+} removal using QG-scaffolded COFs with the removal efficiencies (percentages) depending on (**A**) the amounts of QG-scaffolded COFs 5.0 and (**B**) pH values, which were calculated by the absorbance values of the solutions measured before and after Cu^{2+} removals.

percentage of QG-scaffolded COFs could be achieved at pH 5.0 (Fig. 6B). Importantly, the COFs sorbents could exhibit considerably high absorption efficiency for Cu^{2+} ions, i.e., more than 85% removal, depending on the COFs dosages used and Cu^{2+} amounts in samples.

3.6. Main fluorimetric conditions for Cu^{2+} ions with QG-scaffolded COFs

The main detection conditions of the developed fluorimetric method for Cu^{2+} ions were optimized (Fig. 7). One can see from Fig. 7 that the amounts of QG-scaffolded COFs could exert the large effects on the FL quenching efficiencies when sensing Cu^{2+} ions, showing the maximum one obtained at 4.0 mg mL^{-1} COFs (Fig. 7A). Also, the FL responses of QG-scaffolded COFs to Cu^{2+} ions under different pH conditions were studied, with the data shown in Fig. 7B. Obviously, the optimal pH value for the Cu^{2+} sensing should be at pH 7.0. Furthermore, Fig. 7C shows the effects of ionic strengths on the Cu^{2+} responses of QG-scaffolded COFs. Accordingly, there is no significant effect on the Cu^{2+} responses for the testing media even with NaCl concentrations up to 400 mM, indicating that the electrostatic interaction might hardly influence on the chelating of QG-scaffolded COFs with Cu^{2+} ions. In addition, the response time of QG-scaffolded COFs for Cu^{2+} ions was examined by comparing to pure COFs (Fig. 7D). It was noted that the addition of Cu^{2+} ions could trigger the FL intensities of QG-scaffolded COFs to drop sharply, which would tend to be stable within 2 min. Yet, QG-scaffolded COFs could present a little of faster Cu^{2+} response than pure COFs (Fig. 7D, insert).

3.7. QG-scaffolded COFs-based fluorimetric analysis and removal of Cu^{2+} ions

Under the optimized conditions, the QG-scaffolded COFs-based fluorimetry was directly applied to detect Cu^{2+} ions of different concentrations spiked in blood (Fig. 8). As shown in Fig. 8A, increasing Cu^{2+} concentrations could induce the rationally decreases in the FL intensities of QG-scaffolded COFs. Fig. 8B shows the calibration curve of FL quenching efficiencies versus the logarithms of Cu^{2+} concentrations linearly ranging from 0.0010 to 10.0 μM ($R^2 = 0.9987$), with the limit of detection of about 0.50 nM, estimated by the 3σ rule.

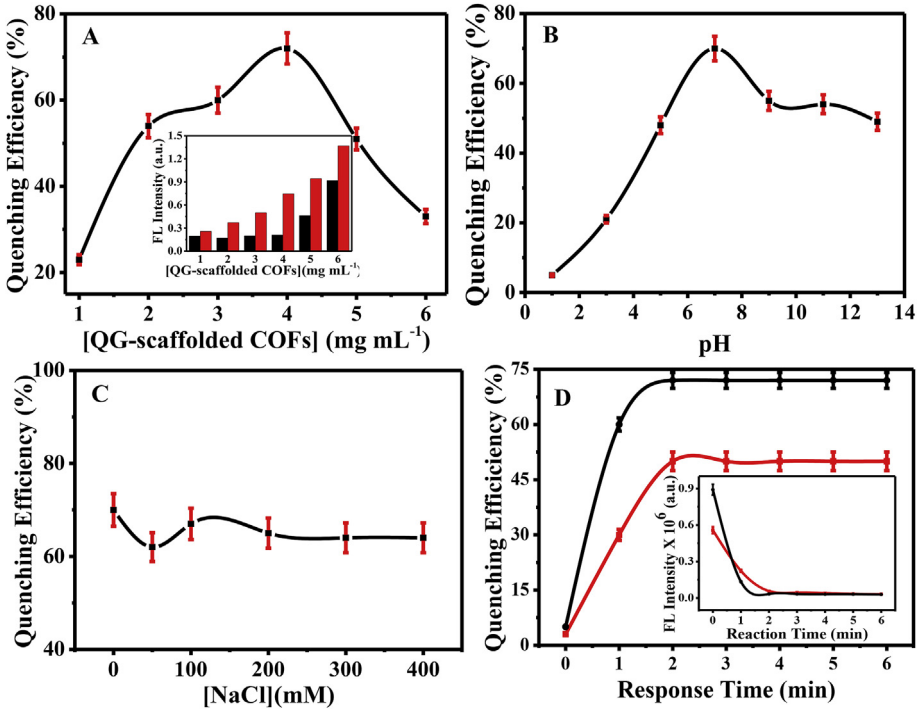

Fig. 7. FL quenching efficiencies of QG-scaffolded COFs depending on (A) QG-scaffolded COFs amounts (insert: FL intensities of QG-scaffolded COFs without (red) and with (black) Cu^{2+} ions), (B) pH values, (C) ion strengths in NaCl concentrations, and (D) response time (insert: FL intensities of QG-scaffolded COFs (black line) and COFs (red line) changing after adding Cu^{2+} ions). (For interpretation of the references to colour in this figure legend, the reader is referred to the Web version of this article.)

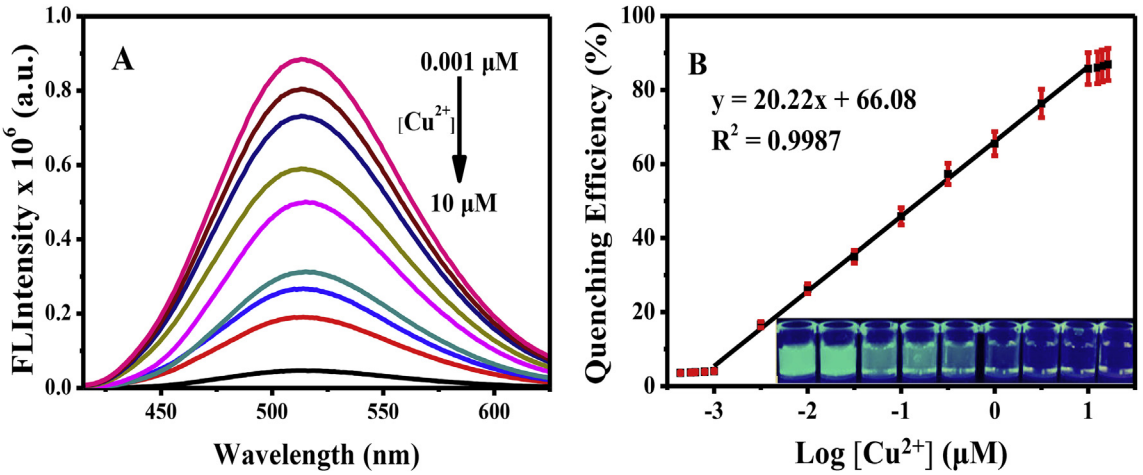

Fig. 8. (A) FL spectra of QG-scaffolded COFs responding to Cu^{2+} ions with different concentrations in blood and (B) the calibration curves of the FL quenching efficiencies versus the logarithmic concentrations of Cu^{2+}ions in blood (insert: photographs of corresponding testing solutions under UV light).

Moreover, the application feasibility of the developed fluorimetric method was investigated for probing Cu^{2+} ions with various levels spiked in wastewater samples (Fig. 9). It can be seen from Fig. 9A that the FL intensities of QG-scaffolded COFs could decrease as increasing Cu^{2+} concentrations. A relationship between the FL quenching efficiencies and the logarithms of Cu^{2+} concentrations was thus obtained (Fig. 9B). Accordingly, Cu^{2+} ions in wastewater could be detected over the linear concentration range of 0.0032−32.0 μM ($R^2 = 0.9894$), with the limit of detection of about 2.4 nM. Therefore, the developed fluorimetry with QG-scaffolded COFs could directly detect Cu^{2+} ions in blood or wastewater samples with considerably high analysis sensitivities.

4. Conclusions

In summary, metal-free QG-scaffolded COFs were successfully synthesized for the first time by the one-step covalent reactions of amine-aldehyde and phenol-aldehyde poly-condensations. It was discovered that hollow QG, which consists of multi-layer graphene and different carbon allotropes having a high proportion of folded edges and surface defects, could endow the scaffoldsed COFs with enhanced FL. Meantime, they could bring the QG-scaffolded COFs with greatly improved environmental stability against any light bleaching and self-quenching in aqueous storage, due to the strong π-π stacking interactions between the hexatomic rings-containing

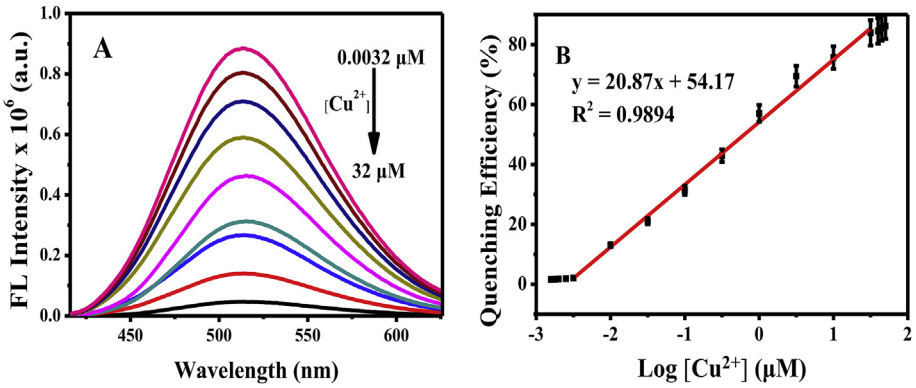

Fig. 9. (A) FL spectra of QG-scaffolded COFs responding to Cu^{2+} ions of different concentrations separately spiked in wastewater and (B) the calibration curves of the FL quenching efficiencies versus the logarithmic concentrations of Cu^{2+}ions.

QG scaffolds and the benzene rings-containing COFs. Moreover, the metal-free MA-PA composites composed in the COFs could possess large surface area and especially rich inherent aminals (−NH−⊖ CH_2−NH−), so that the QG-scaffolded COFs could display the specific binding and powerful absorption capacity for Cu^{2+} ions. Furthermore, the Phen-PA resin of the as-prepared COFs with three-dimensional crosslinking networks might display the fast absorption of Cu^{2+} ions so as to trigger the agglomeration of the COFs probes towards the specific FL quenching. The so developed fluorometry with QG-scaffolded COFs probes could allow for the detection of Cu^{2+} ions separately spiked in blood and wastewater samples, with the Cu^{2+} ions levels down to 0.50 nM and 2.4 nM, respectively. In addition, the yielded QG-scaffolded COFs sorbents could allow for the removal of Cu^{2+} ions in wastewater with pretty high efficiency. More importantly, this hollow QG scaffolds-mediated synthesis route may pave the way toward the fabrication of different kinds of multifunctional metal-free metal-free COFs to be tailored for the applications in biomedical sensing, environmental monitoring, metal removal, organic catalysis, and separation fields.

Declaration of interests

The authors declare that they have no known competing financial interests or personal relationships that could have appeared to influence the work reported in this paper.

Acknowledgment

This work is supported by the National Natural Science Foundations of China (Nos. 21675099, 21375075, and 21601106), and Major Basic Research Program of Natural Science Foundation of Shandong Province, P. R. China (ZR2018ZC0129).

References

[1] R. Uauy, M. Olivares, M. Gonzalez, Essentiality of copper in humans, Nutr. Rev. 45 (1987) 176–180.
[2] M.E. Letelier, A.M. Lepe, M. Faundez, J. Salazar, R. Marin, P. Aracena, et al., Possible mechanisms underlying copper-induced damage in biological membranes leading to cellular toxicity, Chem. Biol. Interact. 151 (2005) 71–82.
[3] X. Hao, P. Xie, Y.G. Zhu, S. Taghavi, G. Wei, C. Rensing, Copper tolerance mechanisms of Mesorhizobium amorphae and its role in aiding phytostabilization by Robinia pseudoacacia in copper contaminated soil, Environ. Sci. Technol. 49 (2015) 2328–2340.
[4] A. Padiglia, R. Medda, A. Bellelli, E. Agostinelli, L. Morpurgo, B. Mondovi, et al., The reductive and oxidative half-reactions and the role of copper ions in plant and mammalian copper-amine oxidases, Eur. J. Inorg. Chem. 2001 (2001) 35–42.
[5] I. Karadjova, B. Izgi, S. Gucer, Fractionation and speciation of Cu, Zn and Fe in wine samples by atomic absorption spectrometry, Spectrochim. Acta B 57 (2002) 581–590.
[6] J.S. Becker, M. Zoriy, A. Matusch, B. Wu, D. Salber, C. Palm, et al., Bioimaging of metals by laser ablation inductively coupled plasma mass spectrometry (LA-ICP-MS), Mass Spectrom. Rev. 29 (2010) 156–175.
[7] M.S. Adams, C.T. Dillon, S. Vogt, B. Lai, J. Stauber, D.F. Jolley, Copper uptake, intracellular localization, and speciation in marine microalgae measured by synchrotronradiation X-ray fluorescence and absorption microspectroscopy, Environ. Sci. Technol. 50 (2016) 8827–8839.
[8] Y. Han, C. Ding, J. Zhou, Y. Tian, Single probe for iImaging and biosensing of pH, Cu(2+) ions, and pH/Cu(2+) in live cells with ratiometric fluorescence signals, Anal. Chem. 87 (2015) 5333–5339.
[9] J. Wang, Q. Zong, A new turn-on fluorescent probe for the detection of copper ion in neat aqueous solution, Sens. Actuators, B 216 (2015) 572–577.
[10] N. Zhang, Y. Si, Z. Sun, L. Chen, R. Li, Y. Qiao, et al., Rapid, selective, and ultrasensitive fluorimetric analysis of mercury and copper levels in blood using bimetallic gold-silver nanoclusters with "silver effect"-enhanced red fluorescence, Anal. Chem. 86 (2014) 11714–11721.
[11] J. Liu, X. Ren, X. Meng, Z. Fang, F. Tang, Sensitive and selective detection of Hg^{2+} and Cu^{2+} ions by fluorescent Ag nanoclusters synthesized via a hydrothermal method, Nanoscale 5 (2013) 10022–10028.
[12] P. Li, X. Duan, Z. Chen, Y. Liu, T. Xie, L. Fang, et al., A near-infrared fluorescent probe for detecting copper(ii) with high selectivity and sensitivity and its biological imaging applications, Chem. Commun. 47 (2011) 7755–7757.
[13] Q. Liu, Z. Tang, B. Ou, L. Liu, Z. Zhou, S. Shen, et al., Design, preparation, and application of ordered porous polymer materials, Mater. Chem. Phys. 144 (2014) 213–225.
[14] A.P. Côté, A.I. Benin, N.W. Ockwig, M. O'Keeffe, A.J. Matzger, O.M. Yaghi, Porous, crystalline, covalent organic frameworks, Science 310 (2005) 1166–1170.
[15] S.Y. Ding, W. Wang, Covalent organic frameworks (COFs): from design to applications, Chem. Soc. Rev. 42 (2013) 548–568.
[16] C. Zhang, J. Luo, A. Yang, M. Jiang, G. Yu, C. Pan, Progress in the application of covalent organic backbone polymers (COFs), Polym. Bull. 2 (2016) 32–39.
[17] M. Pumera, Graphene-based nanomaterials for energy storage, Energy Environ. Sci. 4 (2011) 668–674.
[18] Y. Wang, Y. Shao, D.W. Matson, J. Li, Y. Lin, Nitrogen-doped graphene and its application in electrochemical biosensing, ACS Nano 4 (2010) 1790–1798.
[19] D.A. Brownson, D.K. Kampouris, C.E. Banks, Graphene electrochemistry: fundamental concepts through to prominent applications, Chem. Soc. Rev. 41 (2012) 6944–6976.
[20] H. Wang, S. Li, Y. Si, Z. Sun, S. Li, Y. Lin, Recyclable enzyme mimic of cubic Fe_3O_4 nanoparticles loaded on graphene oxide-dispersed carbon nanotubes with enhanced peroxidase-like catalysis and electrocatalysis, J. Mater. Chem. B 2 (2014), 4442-4428.
[21] H. Wang, S. Li, Y. Si, N. Zhang, Z. Sun, H. Wu, et al., Platinum nanocatalysts loaded on graphene oxide-dispersed carbon nanotubes with greatly enhanced peroxidase-like catalysis and electrocatalysis activities, Nanoscale 6 (2014) 8107–8116.
[22] F. Perreault, A. Fonseca de Faria, M. Elimelech, Environmental applications of graphene-based nanomaterials, Chem. Soc. Rev. 44 (2015) 5861–5896.
[23] M. Li, X. Zhou, S. Guo, N. Wu, Detection of lead (II) with a "turn-on" fluorescent biosensor based on energy transfer from CdSe/ZnS quantum dots to graphene oxide, Biosens. Bioelectron. 43 (2013) 69–74.
[24] Y. Wang, Z. Li, M. Liu, J. Xu, D. Hu, Y. Lin, et al., Multiple-targeted graphene-based nanocarrier for intracellular imaging of mRNAs, Anal. Chim. Acta 983 (2017) 1–8.
[25] E.P. Randviir, D.A. Brownson, M. Gomez-Mingot, D.K. Kampouris, J. Iniesta, C.E. Banks, Electrochemistry of Q-graphene, Nanoscale 4 (2012) 6470–6480.
[26] M. Dong, C. Liu, S. Li, R. Li, Y. Qiao, L. Zhang, et al., Polymerizing dopamine onto

Q-graphene scaffolds towards the fluorescent nanocomposites with high aqueous stability and enhanced fluorescence for the fluorescence analysis and imaging of copper ions, Sens. Actuators, B 232 (2016) 234–242.
[27] M.X. Tan, Y.N. Sum, J.Y. Ying, Y. Zhang, A metal-free poly-melamine-formaldehyde polymer as a solid sorbent for toxic metal removal, Energy Environ. Sci. 6 (2013) 3254–3259.
[28] J.S. West, R.T.V. Fox, Stimulation of Armillaria mellea by phenolic fungicides, Ann. Appl. Biol. 140 (2015) 291–295.
[29] I.M. Kouach, I.H. Pitman, T. Higuchi, Amino acid esters of phenolic drugs as potentially useful prodrugs, J. Pharmacol. Sci. 64 (1975) 1070–1071.
[30] P. Yang, Y. Zhao, Y. Lu, Q.Z. Xu, X.W. Xu, L. Dong, et al., Phenol formaldehyde resin nanoparticles loaded with CdTe quantum dots: a fluorescence resonance energy transfer probe for optical visual detection of copper(II) ions, ACS Nano 5 (2011) 2147–2154.
[31] M.X. Tan, L. Gu, N. Li, J.Y. Ying, Y. Zhang, Metal-free poly-melamine-formaldehyde (mPMF) - a highly efficient catalyst for chemoselective acetalization of aldehydes, Green Chem. 15 (2013) 1127–1132.
[32] S.-R. Guo, J.-Y. Gong, P. Jiang, M. Wu, Y. Lu, S.-H. Yu, Biocompatible, luminescent silver@phenol formaldehyde resin core/shell nanospheres: large-scale synthesis and application for in vivo bioimaging, Adv. Funct. Mater. 18 (2008) 872–879.
[33] G.F. Nordberg, Health hazards of environmental cadmium pollution, Ambio 3 (1974) 55–66.